Available online at www.sciencedirect.com
SCIENCE DIRECT®
Journal of the European Ceramic Society 25 (2005) 3125–3133
www.elsevier.com/locate/jeurceramsoc

Preparation of Al_2O_3–ZrO_2–Ni nanocomposite by pulse electric current and pressureless sintering

W.H. Tuan[a,*], S.M. Liu[a], C.J. Ho[a], C.S. Lin[a], T.J. Yang[b], D.M. Zhang[c], Z.Y. Fu[c], J.K. Guo[d]

[a] *Department of Materials Science and Engineering, National Taiwan University, Taipei, Taiwan*
[b] *Department of Applied Chemistry, Chaoyang University of Technology, Taichung, Taiwan*
[c] *State Key Laboratory of Advanced Technology for Materials Synthesis and Processing, Wuhan University of Technology, Wuhan, China*
[d] *Shanghai Institute of Ceramics, Chinese Academy of Science, Shanghai, China*

Received 31 March 2004; received in revised form 2 July 2004; accepted 10 July 2004
Available online 11 September 2004

Abstract

In the present study, dense Al_2O_3/(ZrO_2 + Ni) nanocomposites are prepared by pulse electric current sintering (PECS) at 1350 °C for 5 min or by pressureless sintering (PLS) at 1600 °C for 1 h. The nanometer-sized Ni particles (∼10 nm) were first introduced into the (Al_2O_3 + ZrO_2) powder mixtures by using a coating technique. The presence of the Ni particles prohibits the coarsening of the composite prepared by PLS; nevertheless, enhances the grain growth of the composites prepared by PECS. The sub-micrometer-sized ZrO_2 particle acts as microstructural stabilizer that slows down the coarsening of matrix grains in the composites prepared by both processes. Due to microstructural refinement, the strength of the Al_2O_3/(5%ZrO_2 + 1%Ni) nanocomposite is ∼40% higher than that of Al_2O_3 alone.

Keywords: Sintering; Nanocomposites; Strength; Al_2O_3; Pulse electric current sintering; Al_2O_3/ZrO_2/Ni

1. Introduction

The applications of ceramics as structural components are restricted because of their poor mechanical performance. To improve the mechanical properties of ceramics has thus attracted much attention. One of the most promising approaches is incorporating a second-phase reinforcement into ceramic matrix.[1] The second-phase reinforcement can be either a ceramic or a metallic phase. The presence of the second-phase inclusions can prohibit the propagation of crack and thus enhance the toughness of ceramics.

Among the many second-phase reinforcements used in previous studies, zirconia particles and nickel particles have received wide attention.[2–4] It is mainly because zirconia and nickel particles are readily available. Furthermore, the addition of either zirconia or nickel particles can enhance both the strength and toughness of ceramics. Recent studies suggested that the toughness of the brittle material can be increased by adding zirconia and metallic particles simultaneously.[5–7] For example, the toughness of an Al_2O_3/(5 vol.% ZrO_2 + 5 vol.% Ni) composite could reach a value as high as 8 MPa $m^{0.5}$.[5] However, the strength of the composite is only marginally enhanced. The size of the Ni inclusions in the composite is relatively large, 2.3 μm. The size may be large enough to induce micro-crack at interface for the presence of thermal expansion mismatch between Al_2O_3 and Ni.[5] By reducing the size of Ni particles to ∼100 nm, the strength of Al_2O_3 may be enhanced significantly.[4] In the present study, both nanometer-sized Ni and submicrometer-sized ZrO_2 powders are added into an Al_2O_3 matrix. The processes of preparing dense Al_2O_3/(ZrO_2 + Ni) nanocomposites are explored. The presence of Ni particles is detrimental to the oxidation resistance of alumina;[8] furthermore, the addition of ZrO_2 above a critical volume fraction, 10 vol.%, can reduce significantly the oxidation resistance of Al_2O_3/(ZrO_2 + Ni) composites,[9] the total amount of (ZrO_2 + Ni) is therefore kept below 10 vol.%.

* Corresponding author. Tel.: +886 2 23659800; fax: +886 2 23634562.
E-mail address: tuan@ccms.ntu.edu.tw (W.H. Tuan).

0955-2219/$ – see front matter © 2004 Elsevier Ltd. All rights reserved.
doi:10.1016/j.jeurceramsoc.2004.07.001

Nanometer-sized Ni powder is needed first to prepare nanocomposites. These nanometer-sized particles have to be dispersed uniformly within the micrometer-sized particles. Furthermore, the coarsening of the nanometer-sized particles during the subsequent high temperature treatment should be as slow as possible. In the present study, a coating technique is used to prepare nanometer-sized nickel particles. The powder mixtures containing nanometer-sized nickel particles are then densified with a pulse electric current sintering (PECS, also known as spark plasma sintering, SPS). The technique is a potential method to prepare nanocomposites for its features of extremely fast heating rate and an external pressure.[10] On top of these features, a pulse electric current is applied simultaneously to the powder compact. The pulse electric current may generate either plasma or electrical discharge between insulating particles. Though the detailed sintering mechanism for PECS is yet to be established, many experimental evidences have demonstrated that the presence of the pulsed electrical field can enhance the densification rate,[10] grain growth rate[11] and creep rate.[12] In the present study, pressureless sintering (PLS) technique was also used to prepare the $Al_2O_3/(ZrO_2 + Ni)$ nanocomposite. The resulting microstructure and the mechanical properties are compared in terms of processing details.

2. Experimental

2.1. Powder preparation

An alumina (TM-DAR, d_{50} = 210 nm, Taimei Chem. Co. Ltd., Tokyo, Japan) powder was mixed with a zirconia (TZ-3Y, ZrO_2 + 3 mol% Y_2O_3, d_{50} = 230 nm, Tosoh Co., Japan) powder by ball milling in de-ionized water for 24 h. Ammonia was added drop by drop into the slurry to reach a pH value of 9.2. A separate solution of nickel nitrate, $Ni(NO_3)_2{\cdot}6H_2O$ (Showa Chem. Co., Japan), was also prepared. The pH value of the nickel nitrate solution was also adjusted to 9.2. The alumina and zirconia slurry was poured into the nickel nitrate solution and then stirred for 30 min. The Ni^{2+} ion could then be absorbed onto the surface of Al_2O_3 particles. The starting amounts of ZrO_2 and Ni added into the slurry were adjusted to result in 5 vol.% each to that of Al_2O_3. The resulting powder mixtures after coating were filtered, washed and dried. The powder mixtures were reduced in pure hydrogen at 550 °C for 1 h, followed by ball milling in ethyl alcohol for 24 h with alumina grinding media. The Al_2O_3 powder, Al_2O_3–ZrO_2 and Al_2O_3–Ni powder mixtures were also prepared with the same technique.

2.2. Pulse electric current sintering (PECS)

The powders were densified in a graphite die with a PECS furnace (Dr. Sinter 1050 SPS, Sumitomo Coal Mining Co., Tokyo, Japan). The electrical pulse with 12:2 pulse sequence, 12 pulses with 3.3 ms for each pulse and followed by 2 periods of zero current, was used. An external pressure of 30 MPa was applied on the powder mixtures from the very beginning of the PECS process. The peak temperature was 1350 °C and the time at the temperature was 1 or 5 min. The heating rate was 130 °C/min, the cooling rate 50 °C/min from 1350 to 600 °C. The final dimensions of the specimen were 20 mm in diameter and around 5–6 mm in thickness.

2.3. Pressureless sintering (PLS)

A uniaxial pressure of 30 MPa was used to prepare the green compacts. The compacts with diameter of 25.4 mm were then sintered within a covered graphite mold at 1600 °C for 1 h. The heating and cooling rates were 5 °C/min. A graphite powder was also used to cover the green compacts. A reducing atmosphere, carbon monoxide mainly, was generated during sintering.

2.4. Characterization

Phase identification was performed by X-ray diffractometry (XRD) with Cu Kα radiation. The amount of Ni in the powder mixtures was determined by using the inductive coupled plasma-atomic emission spectroscopy (ICP-AES, 3000DV, Perkin-Elmer, Optima, USA). The final density of the specimens was determined by the Archimedes method. The solubility between the materials used in the present study was low; the relative density of the composites was estimated by using the theoretical density of 3.98 g/cm^3 for Al_2O_3, 6.05 g/cm^3 for ZrO_2 and 8.90 g/cm^3 for Ni. The microstructure was observed by using scanning electron microscopy (SEM) and transmission electron microscopy (TEM). Polished surfaces were prepared by grinding and polishing with diamond paste to 3 μm and with silica suspension to 0.05 μm. A thermochemical technique[13] was adopted in the present study to reveal the grain boundaries of the composites. The polished specimens were subjected to chemical etching with a solution of 0.8N orthophosphoric acid and 0.5N nitric acid (3:1) for 4–5 min followed by thermal etching at 1250 °C for 30 min. The line intercept technique was used to determine the size of matrix Al_2O_3 grains. More than 200 grains were counted. The size of Ni inclusions in the fired composites was estimated by using the Scherrer formula from XRD patterns.[14]

Before measuring the mechanical properties, the sintered discs were first ground with a 325 grit resin-bonded diamond wheel at depth of 5 μm/pass. The elastic modulus of the specimens was determined with an ultrasonic technique at 5 MHz (Pulser Receiver 5055PR and Oscilloscope 9345CM, LeCoroy Co., USA). The strength of the discs was determined by using a biaxial flexure technique[15] with a universal testing machine (MTS 810, MTS Co., USA). A one-ball-on-three-balls jig was used; the loading rate was 0.5 mm/min. The strength of the discs was calculated by using the following

equations:

$$\sigma_{\max} = \frac{3P}{2\pi t^2}\left[(1+\nu_d)\ln\frac{R_S}{R_C} + \frac{1+\nu_d}{2} + \frac{(1-\nu_d)(2R_S^2 - R_C^2)}{4R_d^2}\right] \quad (1)$$

$$R_C = 0.721\sqrt[3]{PD\left[\frac{1-\nu_b^2}{E_b} + \frac{1-\nu_d^2}{E_d}\right]} \quad (2)$$

In the above equations, P is the applied load, t the thickness of specimens, ν_d the Poisson's ratio of specimens, ν_b the Poisson's ratio of the ball (stainless steel, 0.28 was used in the present study), R_d the radius of specimens, R_S the distance from the center of specimens to the support ball (4.85 mm), R_C the contact radius of the loading ball, D the radius of the loading ball (4.85 mm), E_b the elastic modulus of support balls and E_b the elastic modulus of specimens. The elastic modulus of the specimens, ν_d, was determined by using an ultrasonic method.[5]

The fracture toughness was determined by using an indentation technique at the load of 196 N. The following equations were used to calculate the toughness:[16]

$$K_{IC} = 0.028\left(\frac{E}{H_v}\right)^{0.5} H_v a^{0.5}\left(\frac{c}{a}\right)^{-1.5} \quad (3)$$

$$H_v = 1.8544\frac{P}{(2a)^2} \quad (4)$$

In the above equations, a and c are the half-length of indent and crack. The density variation within the sintered specimen was verified by determining the hardness (H_v) variation within the cross-section of the specimen. The load used for the hardness measurement was 49 N.

3. Results and discussion

3.1. Powder preparation

The Al_2O_3 and ZrO_2 slurry was adjusted to a pH value of 9.2 before the addition of nickel nitrate solution. The surface of Al_2O_3 particles is thus negatively charged first.[17] The adsorption of Ni^{2+} ions onto the surface of Al_2O_3 particles is then possible. After reducing the resulting powder mixtures at 550 °C in hydrogen, metallic nickel particles are formed. Fig. 1 shows the morphology of the Al_2O_3/(ZrO_2 + Ni) powder mixtures. The small particles on the surface of the large particles are Ni particles, as identified by the energy dispersive X-ray spectroscopy. The size of the Ni particles was around 10 nm. The nanometer-sized Ni particles were distributed uniformly on the surface of submicrometer-sized particles. The ZrO_2 content is low; the presence of ZrO_2 particles thus had little effect on the distribution of nanometer-sized Ni particles. The ICP-AES analysis shows that the Ni content

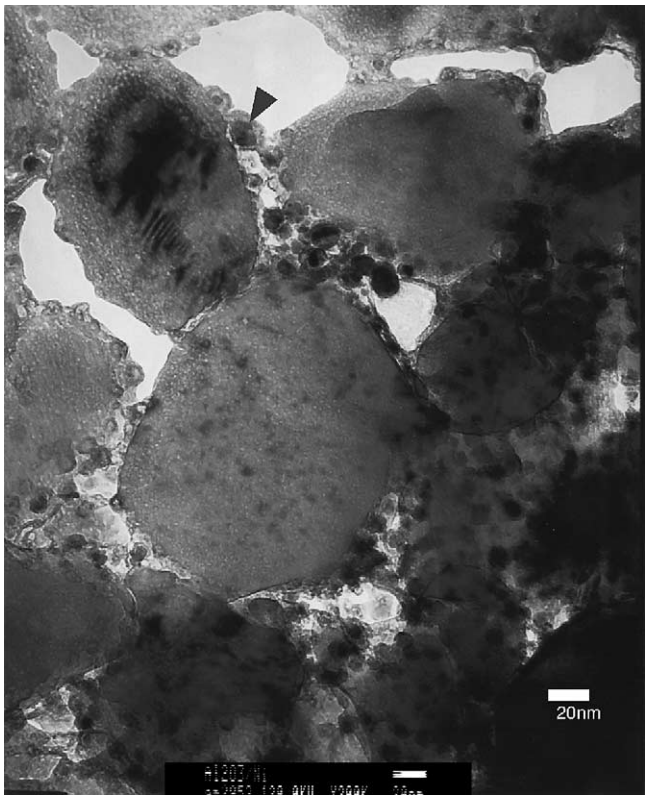

Fig. 1. Morphology of Al_2O_3/(ZrO_2 + Ni) powder mixtures. Arrow indicates a Ni particle.

is lower than the Ni amount added, Table 1. It suggests that only part of the Ni^{2+} ions can be adsorbed onto the surface of Al_2O_3 particles. The excess Ni ions were filtered and washed away. The Ni amount in the powder mixtures was thus much lower than the amount added. The XRD analysis reveals the presence of α-Al_2O_3, t-ZrO_2, Ni and a small amount of m-ZrO_2 in the powder mixture after undergoing reduction in hydrogen, indicating that the reducing atmosphere, pure hydrogen, employed in the present study can transform some t-ZrO_2 to m-ZrO_2.[18]

3.2. Pulse electric current sintering (PECS)

The density of the Al_2O_3/(ZrO_2 + Ni) composite prepared by PECS increases from 96.5% to 99.0% as the time at 1350 °C increases from 1 to 5 min. The microstructures of the composites are shown in Fig. 2. Since the strength of ceramics depends strongly on the amount of porosity, the

Table 1
Composition of Al_2O_3/Ni and Al_2O_3/(ZrO_2 + Ni) powder mixtures after reduction in hydrogen and ball milling as determined by the ICP-AES technique

	Ni (vol.%)	Al_2O_3 (vol.%)	ZrO_2 (vol.%)
Al_2O_3/Ni	0.6	99.4	–
Al_2O_3/(ZrO_2 + Ni)	1.2	93.6	5.2

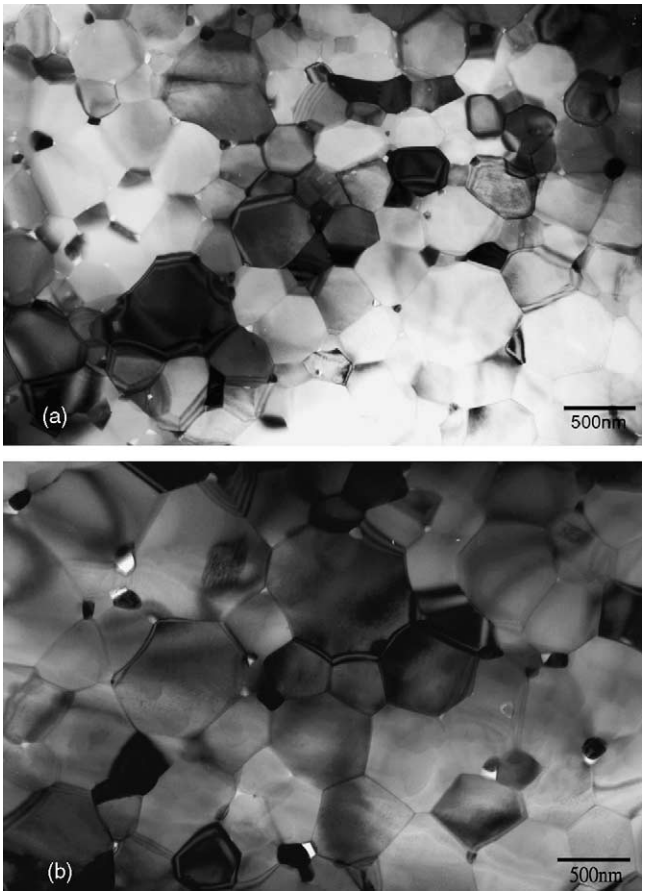

Fig. 2. TEM micrographs of $Al_2O_3/(ZrO_2+Ni)$ composites after PECS at 1350 °C for (a) 1 and (b) 5 min.

PECS was thus carried out at 1350 °C for 5 min to reduce the porosity in the composites.

XRD patterns show no m-ZrO_2 in the zirconia-containing composites, Fig. 3, suggesting that ZrO_2 particles are constrained by the rigid Al_2O_3 matrix after densification. A small amount nickel aluminate spinel, $NiAl_2O_4$, is found in the $Al_2O_3/(ZrO_2 + Ni)$ composite. The presence of spinel suggests that the following reaction has taken place during PECS:

$$2Ni_{(s)} + O_2 + (1 + x)2Al_2O_3 = 2NiO(1 + x)Al_2O_3 \quad (5)$$

The nickel aluminate spinel is a solid solution of $NiAl_2O_4$ and Al_2O_3; the maximum x value varies from 0.27 at 1000 °C to 0.32 at 1300 °C.[19] The existence of $NiAl_2O_4$ suggests that there is a small amount of oxygen dissolved or adsorbed on the surface of nanometer-sized Ni particles after reduction. The extremely fast heating rate used for the PECS leaves little time for the removal of oxygen during heating up stage. The Ni content in the $Al_2O_3/(ZrO_2 + Ni)$ composite is two times that in the Al_2O_3/Ni composite, Table 1. There may be a small amount of $NiAl_2O_4$ in the Al_2O_3/Ni composite prepared by PECS; however, the amount is too low to be detected.

Table 2 shows the relative density of the composites prepared by PECS process. The density of the composites is higher than 99%, demonstrating that the potential of using PECS as an alternative to prepare nanocomposite at a low sintering temperature. Fig. 4 shows the microstructures of the specimens. The size of the matrix grains in the composite is small. The temperature of thermal etching has to be low in order to avoid the coarsening during thermal etching. By combining the chemical etching and thermal etching at

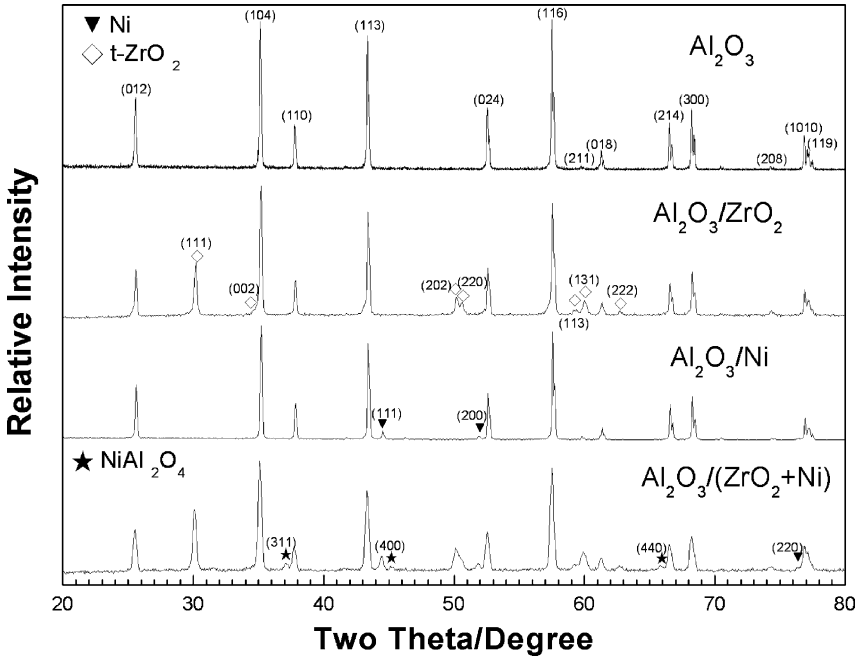

Fig. 3. XRD patterns of the Al_2O_3, Al_2O_3/ZrO_2, Al_2O_3/Ni and $Al_2O_3/(ZrO_2 + Ni)$ specimens after pulse electric current sintering at 1350 °C for 5 min.

Table 2
Density, size of Al_2O_3 matrix grains and Ni inclusions, elastic modulus, strength and toughness of the specimens prepared by pulse electric current sintering

	Relative density (%)	Al_2O_3 grains (μm)	Ni inclusions (nm)	Elastic modulus (GPa)	Strength (MPa)	Toughness (MPa $m^{0.5}$)
Al_2O_3	99.3	1.9	–	407	669 ± 65	2.3 ± 0.1
Al_2O_3/ZrO_2	99.4	0.8	–	392	895 ± 55	2.6 ± 0.1
Al_2O_3/Ni	99.6	2.7	61	397	658 ± 81	2.7 ± 0.2
$Al_2O_3/(ZrO_2 + Ni)$	99.0	0.8	27	397	970 ± 57	2.9 ± 0.1

1250 °C, we could successfully reveal the grain boundaries of the matrix. However, this technique could also remove Ni from the polished surface during chemical etching or thermal etching. The size of Ni was therefore determined by using the XRD technique.

The size of Ni inclusions in the Al_2O_3/Ni and $Al_2O_3/(ZrO_2 + Ni)$ composites is smaller than 100 nm, Table 2, indicating that the Ni-containing composites can be categorized as nanocomposites. However, the size of Al_2O_3 grains in the Al_2O_3/Ni composite was larger than that in the monolithic Al_2O_3 specimen. It seems that the presence of a very small amount of nanometer-sized Ni particles enhances the coarsening of matrix grains in the Al_2O_3/Ni composite. The electrical conducting Ni particles may induce spark or electrical discharge[20] and result in a temperature rise at the locations of Ni particles. Zirconia is an electrical insulator; furthermore, the size of ZrO_2 is much bigger than that of Ni inclusions. The existence of ZrO_2 particles can thus prohibit the coarsening of matrix grains with or without the presence of electric pulse current.

3.3. Pressureless sintering (PLS)

Fig. 5 shows the XRD pattern of the specimens prepared by pressureless sintering. There was no $NiAl_2O_4$ found in the Al_2O_3/Ni and $Al_2O_3/(ZrO_2 + Ni)$ composites, indicating the adsorbed oxygen on the surface of the powder was removed during heating up stage. Table 3 shows the relative density of the composites after pressureless sintering. The density of the $Al_2O_3/(ZrO_2 + Ni)$ composite is higher than 99%, demonstrating that the dense nanocomposite can also be prepared by PLS. Fig. 6 shows the microstructures of the specimens after pressureless sintering. The nanometer-sized Ni and submicrometer-sized ZrO_2 can all prohibit the movement of Al_2O_3 grain boundaries (Table 3).

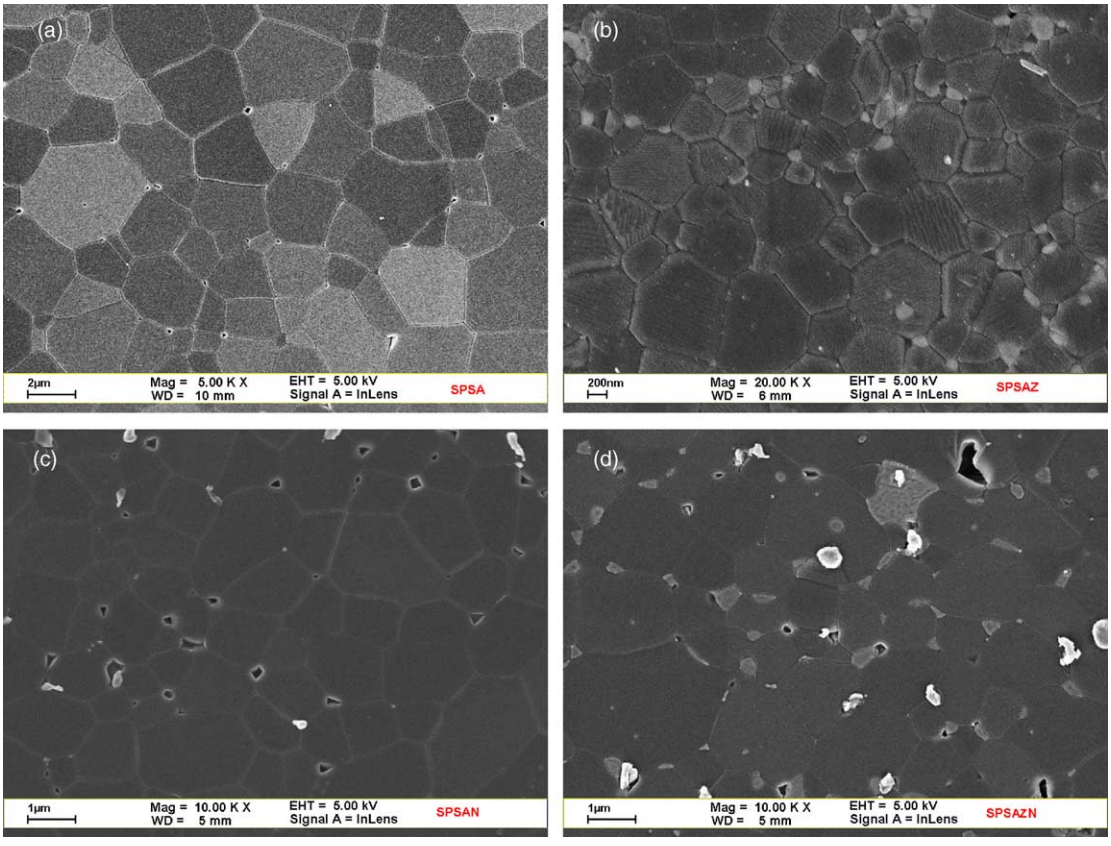

Fig. 4. SEM micrographs of (a) Al_2O_3, (b) Al_2O_3/ZrO_2, (c) Al_2O_3/Ni and (d) $Al_2O_3/(ZrO_2 + Ni)$ specimens after pulse electric current sintering.

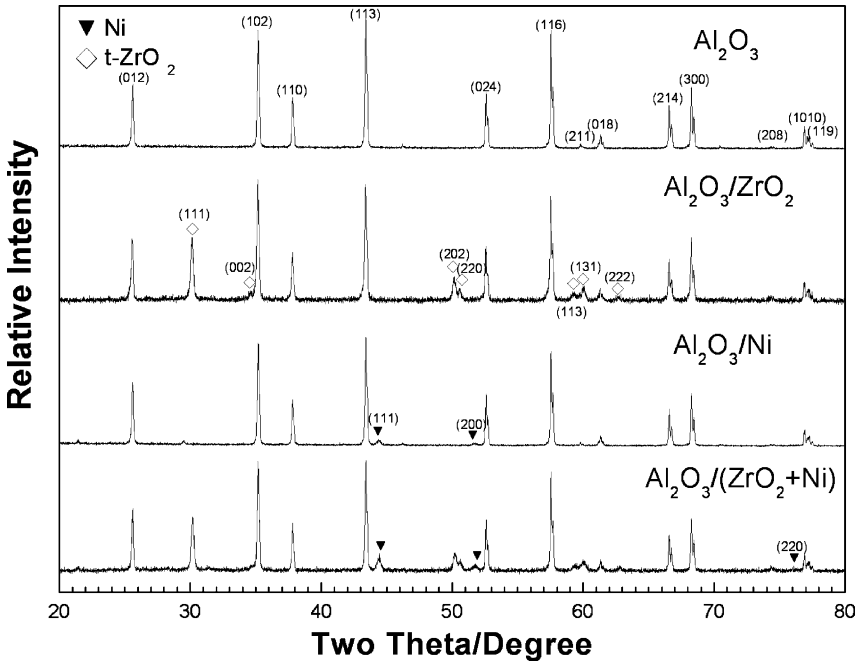

Fig. 5. XRD patterns of the Al_2O_3, Al_2O_3/ZrO_2, Al_2O_3/Ni and $Al_2O_3/(ZrO_2 + Ni)$ specimens after pressureless sintering at 1600 °C for 1 h.

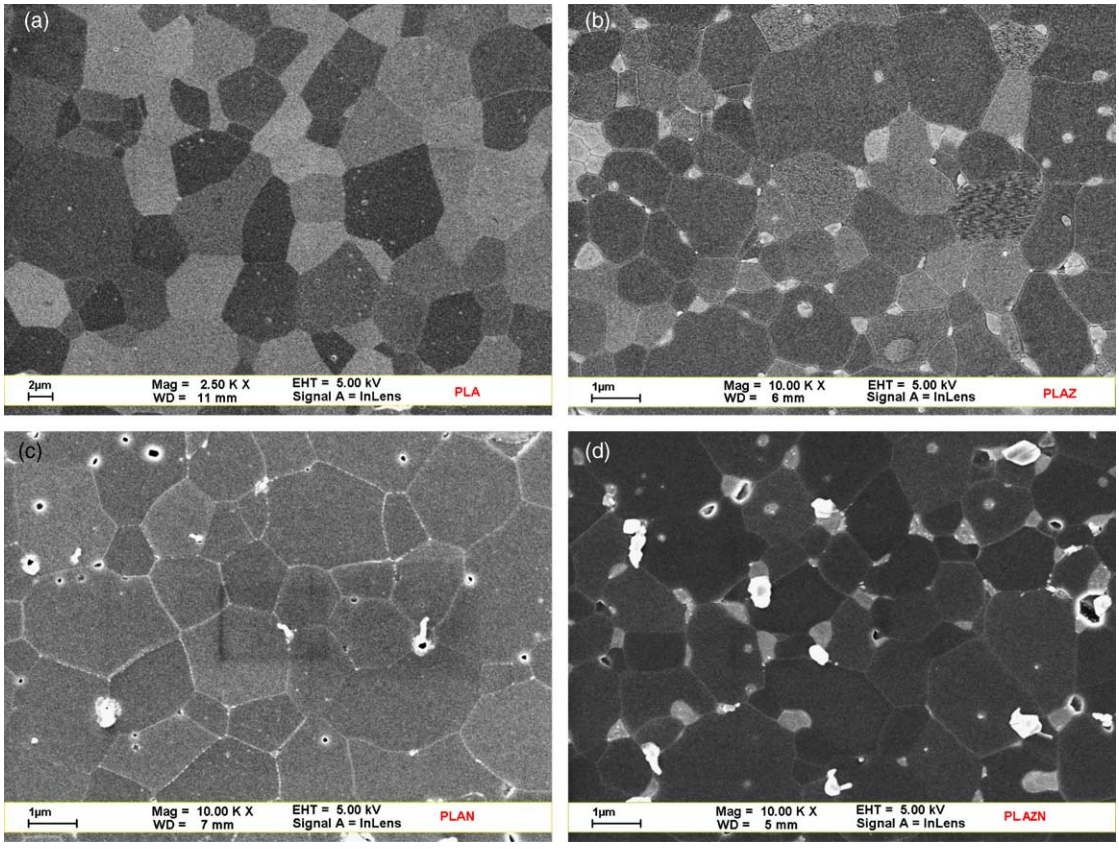

Fig. 6. SEM micrographs of (a) Al_2O_3, (b) Al_2O_3/ZrO_2, (c) Al_2O_3/Ni and (d) $Al_2O_3/(ZrO_2 + Ni)$ specimens after pressureless sintering.

Table 3
Density, size of Al_2O_3 matrix grains and Ni inclusions, elastic modulus, strength and toughness of the specimens prepared by pressureless sintering

	Relative density (%)	Al_2O_3 grains (μm)	Ni inclusions (nm)	Elastic modulus (GPa)	Strength (MPa)	Toughness (MPa $m^{0.5}$)
Al_2O_3	97.1	6.7	–	367	637 ± 15	2.4 ± 0.1
Al_2O_3/ZrO_2	99.8	1.9	–	375	672 ± 40	2.8 ± 0.1
Al_2O_3/Ni	98.8	2.3	62	399	794 ± 57	2.8 ± 0.1
$Al_2O_3/(ZrO_2 + Ni)$	99.4	1.9	32	380	905 ± 25	2.8 ± 0.2

3.4. Comparison

The uniformity of the microstructure can be verified by determining the hardness variation on the cross-section of the composites. Fig. 7 shows the hardness variation as a function of the distance from one edge to the other edge of the Al_2O_3/Ni composite. The green compact of the composite densified by pressureless sintering was prepared by using die-pressing technique. Die pressing usually introduces density variation within the green compact due to the friction between particles and die-wall and between particles.[21] The hardness thus varies within the composite prepared by die-pressing and pressureless sintering. Despite the fact that the die-pressing technique introduces density variation into green compact, the technique has been widely used as the standard technique for the production of engineering ceramics. By taking the hardness variation of the PLS composite as the basis for comparison, the hardness variation within the PECS composite is not any larger. It thus indicates that the PECS can result in a microstructure with acceptable uniformity.

Though the total amount of ZrO_2 and Ni in the $Al_2O_3/(ZrO_2 + Ni)$ nanocomposite is only 6 vol.%; the strength of the composites prepared by PLS and PECS is all 40% higher than that of Al_2O_3 alone. The strengthening effect is independent of the sintering process employed. However, it is worth noting that the strength of the PECS specimens is only 10 to 20% higher than that of the PLS specimens in terms of the same composition.

Fig. 8 shows the strength of all the specimens as a function of the size of Al_2O_3 matrix grains. Similar to monolithic alumina,[22] the strength of composites also decreases with the increase of the size of Al_2O_3 grains. The strengthening effect of the composites can thus be attributed to the microstructural refinement.

3.5. Implications

There are three challenges for the preparation of nanocomposites. The first one is the dispersion of nanometer-sized particles into sub-micrometer sized particles. In the present study, the nanometer-sized Ni particles are prepared by first adjusting the surface charge of Al_2O_3 particles and then coating Ni ion onto their surface. The amount of Ni that can be coated onto the surface of Al_2O_3–ZrO_2 particles is limited by the surface charge available. The amount of Ni particles can be produced onto the surface of Al_2O_3 particles is thus limited. Nevertheless, this technique can produce nanometer-sized particles; furthermore, the distribution of the particles is uniform.

The second challenge is microstructure control. Though the heating rate for the PECS is very fast and the dwell time

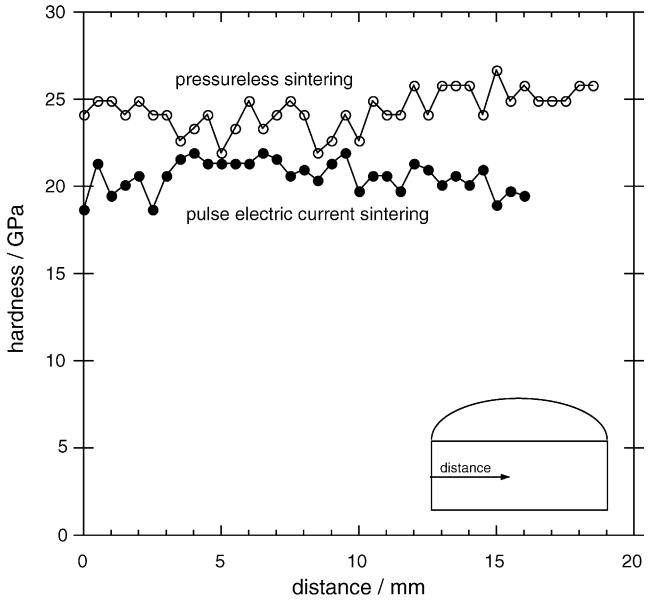

Fig. 7. Hardness variation across one edge to the other one of the cross-section.

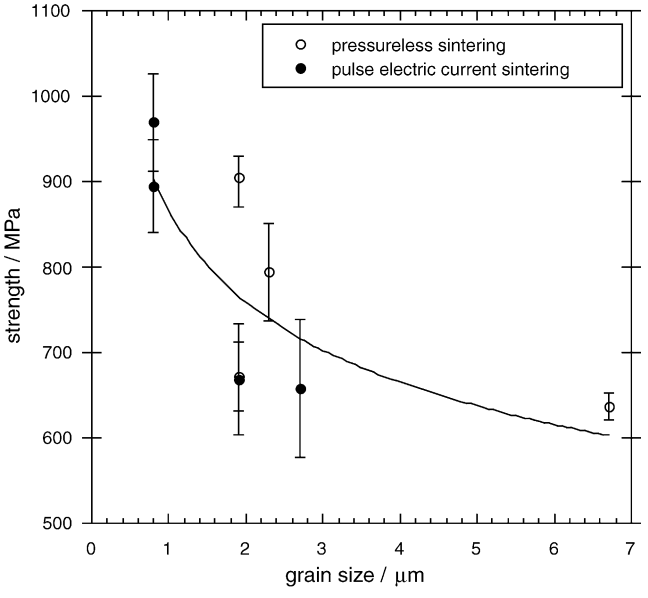

Fig. 8. Strength of all the specimens as a function of the size of matrix grains.

at the peak temperature very short, the amount of porosity can be reduced to a very small amount. Nevertheless, the microstructure undergoes a considerable coarsening within the first few minutes at 1350 °C. For example, the size of Al_2O_3 grains in the $Al_2O_3/(ZrO_2 + Ni)$ nanocomposite increases from 0.31 to 0.8 μm as the dwell time increases from 1 to 5 min (Fig. 2). The extremely fast coarsening rate during PECS has also been noted by Shen et al.[11] In their report, the size of silicon nitride grain increased to 3 times that of the original size within the first 1 min at the PECS temperature. The coarsening rate then slowed down after 2 min. They named the fast coarsening rate as dynamic ripening; they also suggested that further investigation is needed. According to the data provided by the manufacturer, the size of the starting Al_2O_3 powder is 0.2 μm. The Al_2O_3 grains after 1 min at 1350 °C remains more or less the same as that of the starting particles. It seems that there is an incubation period around 1 min at 1350 °C. The coarsening is very fast after this period. The existence of a small amount of nanometer-sized Ni particles can enhance the coarsening of Al_2O_3 matrix during PECS, prohibit the coarsening during PLS. However, the addition of sub-micrometer-sized ZrO_2 particles can always prohibit the growth of Al_2O_3 grains. Therefore, the incorporation of both ZrO_2 and Ni particles seems to be an effective method for microstructural control. Furthermore, the amount of Ni added into the composites is very low. The chance of one Ni inclusion to meet another one is rather remote; the coarsening of Ni is thus limited. Therefore, the pressureless sintering technique can be used to prepare the nanocomposite.

The third challenge is the characterization of the nanocomposite. The grain size of nanocomposite is small. The measurement of grain size is thus a challenging task. The grain size of nanocomposite can be measured by applying transmission electron microscopy technique; however, this technique is time-consuming. The grain size of nanocomposite can be determined easily by using the conventional SEM technique provided a suitable etching technique is available. The usual thermal etching technique may result in biased result because the grain can grow during thermal etching.[23] The temperature of PECS is so low that the temperature of thermal etching has to be even lower. Previous study applied a line intercept technique to determine the grain size from fracture surface.[20] The fracture surface is never flat enough to result in reliable data. In the present study, a thermochemical etching is successfully employed. The thermal temperature is 100 degree lower than that of PECS temperature. The value determined from the TEM micrograph (without etching) and SEM micrograph (with etching) is consistent to each other. The coarsening during the thermochemical treatment is therefore negligible. Many previous studies on the ceramics prepared by PECS process seldom reported their mechanical properties. Furthermore, the sparse data show significant scatter.[24] It may all reflect the fact that the PECS specimens may be not uniform as the size of specimens is larger than 20 mm. In the present study, a biaxial flexure technique is used to determine the strength of spherical discs. The scatter of the strength data is relatively small, indicting that the uniformity of the microstructure of the nanocomposites prepared in the present study is acceptable. Furthermore, all the composites are tested with the same configuration. The comparison between the monolithic specimen and composite can still shed light on the evaluation of processing parameters. Therefore, the biaxial flexure technique can deliver a quick and reliable method to evaluate the strength of PECS specimens.

For the $Al_2O_3/(ZrO_2 + Ni)$ micro-composites, the toughening mechanisms which are active in the composite can interact with each other;[25] such as that the extent of phase transformation of ZrO_2 particles was enhanced due to the presence of Ni particles; the existence of ZrO_2 increased the ductility Ni particles. However, the amount of Ni in the $Al_2O_3/(ZrO_2 + Ni)$ nanocomposite prepared in the present study is only 1 vol.%, the interactions between the two toughening mechanisms may therefore small. The toughness enhancement of the composite is therefore marginal.

4. Conclusions

In the present study, dense $Al_2O_3/(ZrO_2 + Ni)$ nanocomposites are prepared by pressureless sintering and pulse electric current sintering. The strength and toughness of the nanocomposite are all higher than those of alumina alone in terms of the same processing conditions. The size of the PECS specimens is traded off by its extremely fast heating rate. In the present study, two reliable characterization techniques have been used to characterize the microstructure and the strength of the nanocomposite. A thermochemical etching technique can be used to reveal the grain boundaries of matrix at a rather low temperature; biaxial 4-ball flexure technique to determine the strength. These two techniques are valuable especially for the assessment of nanocomposite.

The present study also demonstrates that nanometer-sized Ni particles can be distributed uniformly onto the surface of Al_2O_3 particles by employing a coating technique. As long as both ZrO_2 and Ni particles are incorporated simultaneously into Al_2O_3 matrix, the coarsening of matrix grains is constrained. Due to the coarsening during sintering is limited by the addition of the inclusions; the nanocomposite can also be prepared by pressureless sintering.

Acknowledgments

The National Science Council supported the present study through the contract number of NSC90-2216-E002-034.

References

1. Evans, A. G., Perspective on the development of high-toughness ceramics. *J. Am. Ceram. Soc.*, 1990, **73**, 187–206.

2. Hannink, R. H. J., Kelly, P. M. and Muddle, B. C., Transformation toughening in zirconia-containing ceramics. *J. Am. Ceram. Soc.*, 2000, **83**, 461–487.
3. Tuan, W. H. and Brook, R. J., Processing of alumina/nickel composites. *J. Eur. Ceram. Soc.*, 1992, **10**, 95–100.
4. Sekino, T., Nakajima, T., Ueda, S. and Niihara, K., Reduction and sintering of a nickel-dispersed-alumina composite and its properties. *J. Am. Ceram. Soc.*, 1997, **80**, 1139–1148.
5. Chen, R. Z., Chiu, Y. T. and Tuan, W. H., Toughening alumina with both nickel and zirconia inclusions. *J. Eur. Ceram. Soc.*, 2000, **20**, 1901–1906.
6. Sbaizero, O., Roitti, S. and Pezzotti, G., R-curve behavior of alumina toughened with molybdenum and zirconia particles. *Mater. Sci. Eng.*, 2003, **A359**, 297–302.
7. Li, M. and Soboyejo, W. O., Synergistic toughening of a hybrid NiAl composite reinforced with partially stabilized zirconia and molybdenum particles. *Mater. Sci. Eng.*, 1999, **A271**, 491–495.
8. Wang, T. C., Chen, R. Z. and Tuan, W. H., Oxidation resistance of Ni-toughened Al_2O_3. *J. Eur. Ceram. Soc.*, 2003, **23**, 927–934.
9. Wang, T. C., Chen, R. Z. and Tuan, W. H., Effect of zirconia addition on the oxidation resistance of Ni-toughened Al_2O_3. *J. Eur. Ceram. Soc.*, 2004, **24**, 833–840.
10. Wang, S. W., Chen, L. D. and Hirai, T., Densification of Al_2O_3 powder using spark plasma sintering. *J. Mater. Res.*, 2000, **15**, 982–987.
11. Shen, Z., Zhao, Z., Peng, H. and Nygren, M., Formation of tough interlocking microstructures in silicon nitride ceramics by dynamic ripening. *Nature*, 2002, **417**, 266–269.
12. Shen, Z., Peng, H. and Nygren, M., Formidable increase in the superplasticity of ceramics in the presence of an electric field. *Adv. Mater.*, 2003, **15**, 1006–1009.
13. Owate, I. and Freer, R., Thermochemical etching method for ceramics. *J. Am. Ceram. Soc.*, 1992, **75**, 1266–1268.
14. Cullity, B. D., *Element of X-Ray Diffraction* (*2nd ed.*). Addison-Wesley Publication Co. Inc., Reading, 1978 p. 101.
15. Shetty, D. K., Rosenfield, A. R., McGuire, P., Bansal, G. K. and Duckworth, W. H., Biaxial flexure tests for ceramics. *Am. Ceram. Soc. Bull.*, 1980, **59**, 1103–1107.
16. Lawn, B. R., Evans, A. G. and Marshall, D. B., Elastic/plastic indentation damage in ceramics: the median/radial crack systems. *J. Am. Ceram. Soc.*, 1984, **63**, 574–580.
17. Tuan, W. H., Wu, H. H. and Yang, T. J., The preparation of Al_2O_3/Ni composites by a powder coating technique. *J. Mater. Sci.*, 1995, **30**, 855–859.
18. Hsieh, H. G. and Tuan, W. H., Exaggerated grain growth in a yttria-containing zirconia ceramic. *J. Mater. Sci. Lett.*, 2002, **21**, 391–393.
19. Trumble, K. P. and Ruehle, M., The thermodynamics of spinel interphase formation at diffusion-bonded Ni/Al_2O_3 interfaces. *Acta Metall.*, 1994, **39**, 1915–1924.
20. Shen, Z., Johnsson, M., Zhao, Z. and Nygren, M., Spark plasma sintering of alumina. *J. Am. Ceram. Soc.*, 2002, **85**, 1921–1927.
21. Welzen, J. T. A. M., Die compaction of ceramic powders. *J. Mater. Educ.*, 1986, **8**, 187–238.
22. Tuan, W. H., Lai, M. J., Lin, M. C., Chan, C. C. and Chiu, S. C., The mechanical performance of alumina as a function of grain size. *Mater. Chem. Phys.*, 1994, **36**, 246–251.
23. Chen, R. Z. and Tuan, W. H., Thermal etching of alumina. *Am. Ceram. Soc. Bull.*, 2000, **79**, 83–86.
24. Jayaseelan, D. D., Kondo, N., Rani, D. A., Ueno, S., Ohji, T. and Kanzaki, S., Pulse electric current sintering of Al_2O_3/3 vol.%ZrO_2 with constrained grains and high strength. *J. Am. Ceram. Soc.*, 2002, **85**, 2870–2872.
25. Tuan, W. H. and Chen, R. Z., Interactions between toughening mechanisms: transformation toughening vs. plastic deformation. *J. Mater. Res.*, 2002, **17**, 2921–2928.